Stellar populations in the fields surrounding the LMC clusters NGC 2154 and NGC 1898

E. Chiosi,[1]* G. Baume,[2] G. Carraro,[3,4] E. Costa[5] and A. Vallenari[1]

[1] *INAF, Osservatorio Astronomico di Padova, Vicolo Osservatorio 2, I-35122 Padova, Italy*
[2] *Facultad de Ciencias Astronómicas y Geofísicas (UNLP), Instituto de Astrofísica de la Plata (CONICET,UNLP), Paseo del Bosque s/n, La Plata, Argentina*
[3] *ESO, Alonso de Cordova 3107, Santiago de Chile, Chile*
[4] *Dipartimento di Astronomia, Universitá di Padova, Vicolo Osservatorio 3, I-35122 Padova, Italy*
[5] *Departamento de Astronomía, Universidad de Chile, Casilla 36-D, Santiago, Chile*

ABSTRACT

In this paper we present a study and comparison of the star formation rates (SFRs) in the fields around NGC 1898 and NGC 2154, two intermediate-age star clusters located in very different regions of the Large Magellanic Cloud (LMC). We also derive ages for NGC 1898, and seven minor clusters which happen to fall in the field of NGC 1898, for which basic parameters were previously unknown. We do not focus on NGC 2154, because this cluster was already investigated by Baume et al. The ages of the clusters were derived by means of the isochrone fitting method on their *clean* colour–magnitude diagrams. Two distinct populations of clusters were found: one cluster (NGC 2154) has a mean age of 1.7 Gyr, with indication of extended star formation over roughly a 1 Gyr period, while all the others have ages between 100 and 200 Myr. The SFRs of the adjacent fields were inferred using the downhill-simplex algorithm. Both SFRs show enhancements at 200, 400, 800 Myr, and at 1, 6 and 8 Gyr. These bursts in the SFR are probably the result of dynamical interactions between the Magellanic Clouds (MCs), and between the MCs and the Milky Way.

Key words: Magellanic Clouds – galaxies: star clusters: individual: NGC 2154, NGC 1898 – galaxies: stellar content.

1 INTRODUCTION

Stellar clusters have traditionally been considered as the natural cradle of stars, from which stars can migrate into the field (Lada & Lada 2003). However we cannot exclude the possibility that stars also form in the field itself (Bressert et al. 2010). To evaluate the statistical significance of stars formed in situ among field populations, it is necessary to make detailed comparative studies (including ages) of many clusters and their related fields. The Magellanic Clouds (MCs) are located close to the Galaxy (at about 60 kpc), their members can be considered essentially equidistant and they present a rich population of clusters. Therefore they provide an ideal laboratory to address this matter.

In this paper we present an analysis of the star formation rate (SFR) in the *fields* around two populous stellar clusters of the LMC: NGC 1898, located in the central LMC bar, and NGC 2154, located in the NE of the Large Magellanic Cloud (LMC) as shown in Fig. 1. We also present a photometric study of NGC 1898, and of seven minor clusters which happen to fall in the field of NGC 1898, for

which basic parameters are so far unknown. We note that NGC 2154 was subject of a previous study by our group, using the same theoretical tools (Baume et al. 2007, hereafter Bau07).

The above sample is particularly interesting for it comprises both disc and bar populations that are recognized to have different star formation histories (SFHs), as discussed by Vallenari et al (1994) and Harris et al (2009). Holtzman et al. (1999) find, based on HST data, that there is a significant component of stars older than 4 Gyr in the outer fields and in the bar. They also note that there is no age gap in the field SFR, unlike the case of the cluster SFR. Olsen (1999) analyse six fields in the LMC and find that all of them have significant recent (< 3–4 Gyr) star formation. They find that bar fields experience more star formation in the range of 4–8 Gyr than disc fields. Among other works we mention a recent study on the LMC SFH by Rubele et al. (2012) based on vista data. They analyse the SFH in several regions of the LMC. In particular their tile 6–6 contains NGC 1898 and tile 8–8 contains NGC 2154. They find a continuous SF in the bar (NGC 1898) while some burst can be recognized in the disc area (NGC 2154) at 20 Myr, 1–2 Gyr and 8 Gyr.

The paper is structured as follows: in Section 2 we summarize the observations and the data reduction procedures, in Section 3 we

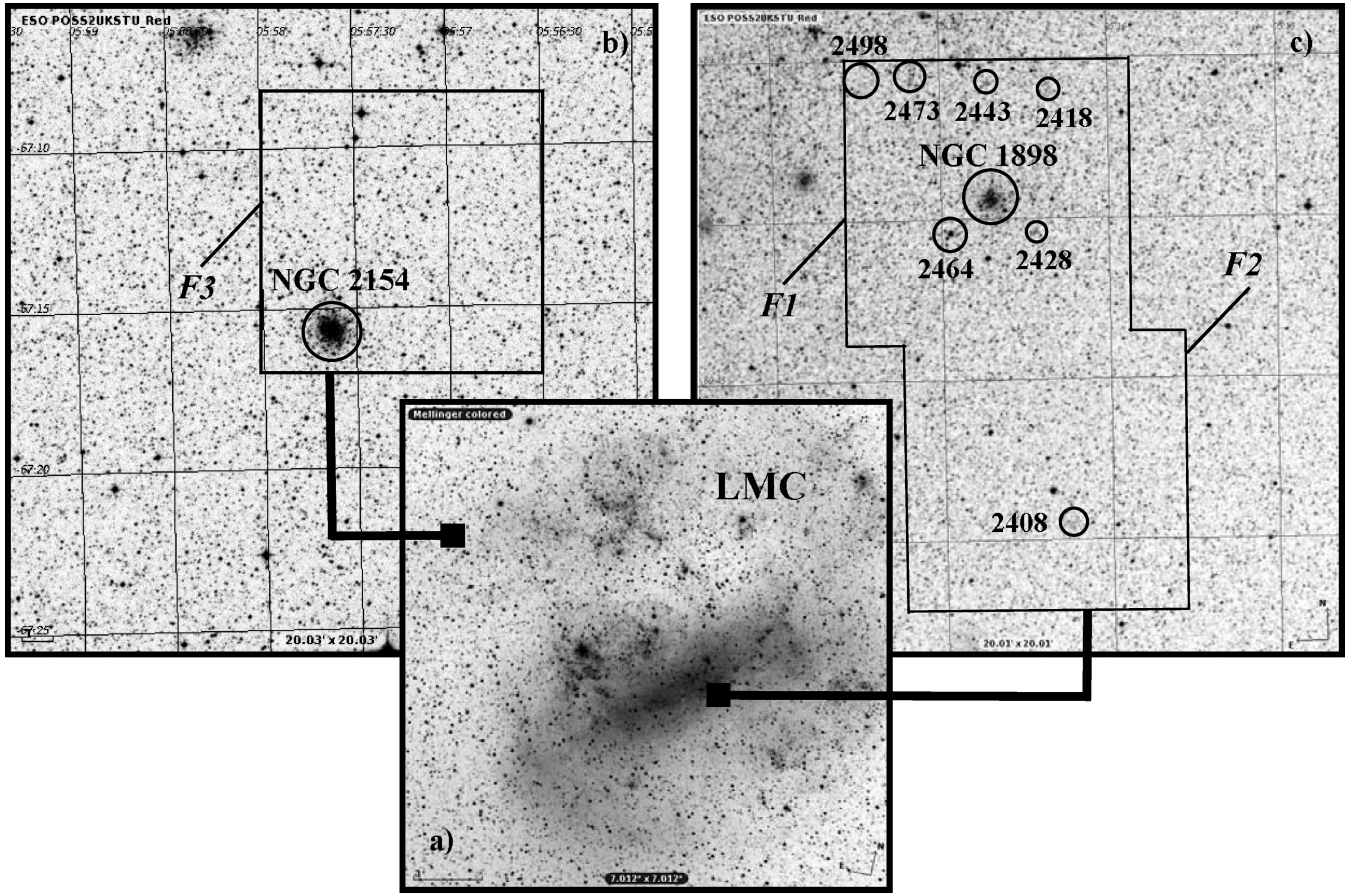* E-mail: emanuela.chiosi@oapd.inaf.it

Figure 1. Upper panels (b) and (c) show the 8.85 arcmin × 8.85 arcmin areas surveyed by our *BR* observations (*F*1, *F*2 and *F*3), superimposed on approximately 20.0 arcmin × 20.0 arcmin DSS-2 red images. We note that fields *F*1 and *F*2 have a very small overlap (∼15 arcsec), which is not noticeable in panel (c). The circles in them depict the location and approximate size of the star clusters studied. North is at the top and East is to the left. Lower panel (a) shows the location of our fields in the LMC.

describe the methods used for the SFR, in Section 4 we present the main results for the two fields and in Section 5 we present the cluster analysis. Finally, in Section 6, we summarize the conclusions of our analysis.

2 OBSERVATIONS AND DATA REDUCTION

In the following we describe the observation and data reduction procedure for the NGC 1898 field. For the equivalent description of the field of NGC 2154 we refer to Bau07.

Our study is based on $B(R)_{KC}$ observations carried out using a 24μ pixel Tektronix 2048 × 2048 detector attached to the Cassegrain focus of the du Pont 2.5-m telescope at Las Campanas Observatory, Chile. Gain and read noise were 3 e^-/ADU and 7 e^-, respectively. This set-up provided direct imaging over a field of view (FOV) of 8.85 arcmin × 8.85 arcmin with a scale of 0.259 arcsec pixel^{-1}. This relatively large FOV allowed us to study a good sample of the LMC field population around the clusters. A log of the observations is given in Table 1. Seeing varied between 0.9 and 1.5 arcsec. A log of the observations for NGC 2154 can be found in table 1 of Bau07.

The observations presented in this paper were secured as a part of a large survey to study the SFH and absolute proper motion of the MCs (Noël et al. 2007, 2009; Costa et al. 2009, 2011).

All frames were processed using standard IRAF tasks. We used the CCDRED package for the pre-reduction procedure, for which purpose

Table 1. Logfile of observations in the area of NGC 1898, together with the coefficients used in our transformation equations (1) and (2).

Field	Filter	Date	Airmass	Exptime (s)
		2007 Oct. 10	1.37	60
*F*1	*B*	2007 Oct. 10	1.37	800
		2008 Oct. 28	1.36	6 × 800
		2007 Oct. 10	1.39	120
*F*1	*R*	2007 Oct. 10	1.38	600
		2007 Oct. 06	1.36	10 × 450
		2007 Oct. 10	1.34	60
*F*2	*B*	2007 Oct. 10	1.34	800
		2008 Oct. 29	1.35	8 × 800
		2007 Oct. 10	1.36	120
*F*2	*R*	2007 Oct. 10	1.35	600
		2007 Oct. 09	1.35	17 × 500

Transformation coefficients

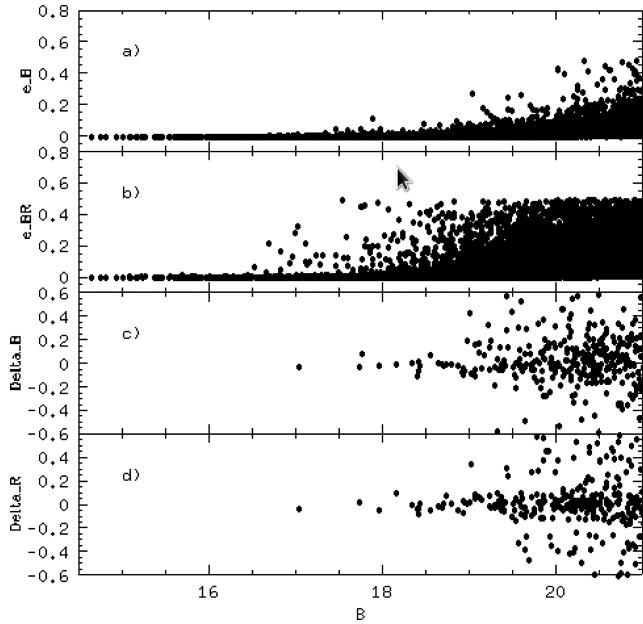|	
$b_1 = 1.058 \pm 0.025$	$r_1 = 0.613 \pm 0.049$
$b_2 = 0.213 \pm 0.019$	$r_2 = 0.136 \pm 0.038$
$b_3 = -0.043 \pm 0.005$	$r_3 = -0.009 \pm 0.007$

Figure 2. Panels (a) and (b): photometric errors (from DAOPHOT) in B and $(B - R)$, plotted as a function of the B magnitude. Panels (c) and (d): comparison of the photometry in fields $F1$ and $F2$, based on their overlapping region.

zero exposures and sky flats were taken every night. PSF instrumental magnitudes were obtained in the standard way using the DAOPHOT package (Stetson 1987), and the DAOMASTER code (Stetson 1992) was used to combine the corresponding photometric tables for different exposure times and/or filters. Our instrumental photometry was calibrated using the PHOTCAL package, for which purpose we observed several *UBVRI* standard star areas (Landolt 1992; namely fields Mark A, PG0231+051, PG2213-006, SA098, SA110, SA113 and TPhe), and performed aperture photometry on them.

Our transformation equations were

$$b = B + b_1 + b_2 X + b_3(B - R) \qquad (1)$$

$$r = R + r_1 + r_2 X + r_3(B - R). \qquad (2)$$

In these equations b and r are the instrumental magnitudes normalized to 1 s, and X is the airmass. The values of the transformation coefficients in the above equations are also listed in Table 1. The rms of the fits in the blue and red bands turned out to be 0.026 and 0.036, respectively.

Our photometric errors (from DAOPHOT) in B and $(B - R)$ are plotted as a function of the B magnitude in panels (a) and (b) of Fig. 2. Given that there is a very small overlap between fields $F1$ and $F2$ (not obvious in Fig. 1), it was possible to compare the photometry secured in each of them. The differences $Delta_B$ and $Delta_R$ as a function of B are plotted in panels (c) and (d) of Fig. 2.

2.1 COMPLETENESS

The definition of photometric completeness is of fundamental importance for cluster analysis and for the reconstruction of stellar populations used in the determination of SFH. The procedure for completeness determination is well described in Bau07 and substantially is based on the injection in the image of a suitable number of artificial stars of known magnitude and position. The number of recovered artificial stars through the complete data reduction

Table 2. Completeness study for the NGC2154 and NGC1898 regions: cluster and field.

$Delta_B$	NGC2154		NGC1898	
	Cluster	Field	Cluster	Field
16.0–16.5			100 per cent	100 per cent
16.5–17.0			100 per cent	100 per cent
17.0–17.5			97 per cent	100 per cent
17.5–18.0			93 per cent	100 per cent
18.0–18.5			83 per cent	100 per cent
18.5–19.0			74 per cent	100 per cent
19.0–19.5			59 per cent	100 per cent
19.5–20.0	100 per cent	100 per cent	55 per cent	100 per cent
20.0–20.5	93 per cent	100 per cent	56 per cent	100 per cent
20.5–21.0	75 per cent	100 per cent	42 per cent	96 per cent
21.0–21.5	57 per cent	100 per cent	30 per cent	86 per cent
21.5–22.0	57 per cent	100 per cent	31 per cent	77 per cent
22.0–22.5	56 per cent	100 per cent	23 per cent	62 per cent
22.5–23.0	55 per cent	100 per cent	24 per cent	53 per cent
23.0–23.5	54 per cent	83 per cent	16 per cent	40 per cent
23.5–24.0	42 per cent	61 per cent	12 per cent	33 per cent
24.0–24.5	29 per cent	62 per cent	8 per cent	20 per cent
24.5–25.0	32 per cent	67 per cent		
25.0–25.5	35 per cent	82 per cent		
25.5–26.0	36 per cent	50 per cent		

pipeline over the initial number per magnitude interval constitutes the completeness coefficient for that interval. We summarize the main results for completeness in the NGC 2154 and NGC 1898 cluster and field areas in Table 2.

A byproduct of the completeness analysis is an additional estimate of the photometric errors, independent from DAOPHOT, obtained by comparing ADDSTAR input and output magnitudes. From our experiments we found that the difference between injected and extracted B and R magnitudes is larger than the DAOMASTER photometric errors only for B and R fainter than about 24 mag. DAOMASTER combines in quadrature photometric errors from single images, and therefore provides a statistically reliable error estimate. We will use DAOMASTER photometric errors in this paper.

3 METHODS TO STUDY THE FIELD SFR

In order to derive the field SFR in the regions of NGC 2154 and NGC 1898, we must first subtract the clusters from the corresponding fields. In the case of NGC 2154, we removed the area within a radius of 500 pixels from the cluster centre. This area extends well outside the core radius of NGC 2154 ($a = 14.7$ arcsec, about 57 pixels), as was determined from the fit with Elson profiles made by Bau07. In the case of NGC 1898 a radius of 300 pixels was adopted.

The field SFR is then obtained comparing the observed field colour–magnitude diagram (CMD) with synthetic CMDs, by means of a minimization algorithm.

The first step involves creating a set of synthetic stellar populations, and a grid to be applied to the CMDs. The former were created using the Bertelli ZVAR code release, based on the Girardi et al. (2000) set of evolutionary tracks.

The above code needs a set of parameters which must be tuned to the specific case in question. In particular, we need to assume an age–metallicity relation and an initial mass function (IMF). The age–metallicity relation was adopted from Pagel & Tautvaisiene (1998) and is summarized in Table 3. The adopted IMF was that of Kroupa (2002), which is a power law function with a slope of

Table 3. Age–metallicity relation adopted in the ZVAR code for our LMC fields. From Pagel & Tautvaisiene (1998).

Age interval (yr)	Metallicity Z
6.3e7:2e8	0.010
2e8:3e8	0.010
3e8:4e8	0.010
4e8:5e8	0.010
5e8:6e8	0.007
6e8:8e8	0.007
8e8:1e9	0.007
1e9:2e9	0.005
2e9:3e9	0.004
3e9:4e9	0.004
4e9:5e9	0.003
5e9:6e9	0.003
6e9:8e9	0.003
8e9:1e10	0.002
1e10:1.2e10	0.002

Figure 4. CMD of the region observed in the vicinity of NGC 1898, with the superimposed grid.

Figure 3. CMD of the region observed in the vicinity of NGC 2154, with the superimposed grid.

$x = 2.3$, for stellar masses $M > 0.5\,M_\odot$, and of $x = 1.3$ for the 0.08–0.5 $M_\odot$ mass range.

We generate populations of 12 000 stars for each age interval, covering a range of ages from a few Myr to 10 Gyr. The stars were distributed according to the IMF from brightest to faintest, down to the magnitude limit set by completeness.

The grids applied to the CMDs (see Figs 3 and 4: GRID 2154 and GRID 1898) were built in a way that enhances the most important evolutionary stages. A fine binning was used along the main sequence in order to resolve the different turn-offs of the contributing populations, while a coarser division was adopted for the red clump and sub-giant branch regions. This last feature reflects the
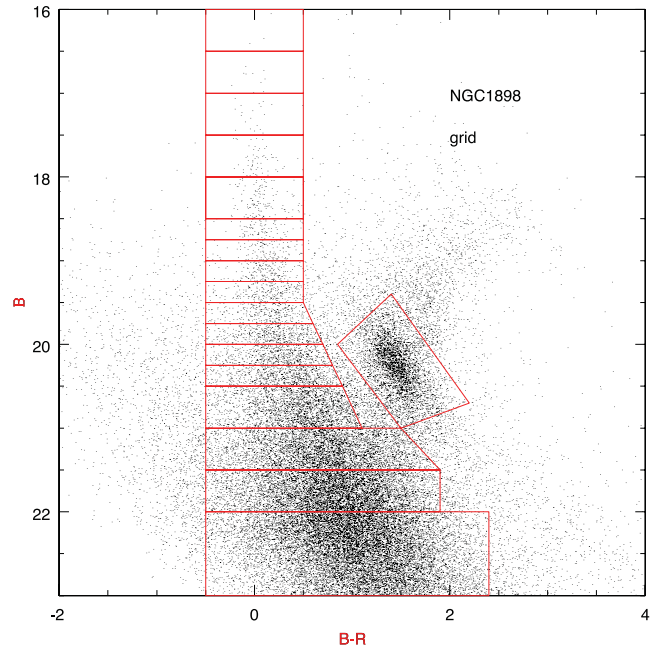
uncertainties resulting from both the experimental procedure and the theoretical models.

A key point in the simulation is the completeness and photometric error reproduction. Both aspects were considered in the algorithm to generate the synthetic populations, as explained in the next paragraph. They turn out to be particularly critical in the case of NGC 1898 where the photometric errors are larger at brighter magnitudes than in the case of NGC 2154. We note that the 50 per cent completeness limit settles at $B \simeq 23$ corresponding to the turn-off of a population of 6.3 Gyr. The determination of the SFH for ages older than this limit is therefore largely uncertain and degenerate in the case of NGC 1898 but older populations are needed to fill the red clump bin. In the case of NGC 2154, we refer the reader to Bau07 for a discussion of the photometric errors and completeness. We note that for this cluster the completeness limit settles at $B \simeq 25.5$ well below the turn-off of a population of 10 Gyr.

Having created the synthetic populations and the grid, we are in a position to generate histograms (i.e. number of stars falling in each sector of the CMD), both for the single theoretical stellar populations and for the data. At this stage, we need to introduce photometric errors in the stellar models and apply a completeness correction to the theoretical populations. We also need to apply a reddening correction, and adopt a distance modulus for the LMC. Following Westerlund (1997), we have used a reddening of $E(B - V) = 0.08$ and a distance modulus of 18.5.

The overall theoretical population is the sum of the subpopulations generated for each age interval, multiplied by a coefficient. We determine the best set of coefficients weighting the theoretical histograms that best reproduce the observational histogram. To this aim we made use of the downhill simplex method of optimization (Nelder & Mead 1965).The downhill simplex acts as a probe moving in an N-parameter space, where N is the number of theoretical subpopulations and therefore of coefficients. Its shape in the N-parameter space is defined by $N + 1$ initial points. It starts calculating at a given point the χ^2 function set by the sum of the

squared differences between the corresponding bins of the theoretical histogram resulting from the given mixture and the observational histogram. Then it moves to another point through reflection and again calculates χ^2, and so on; resizing and reflecting it can define a gradient of the χ^2 in coefficient space and following this gradient it rapidly converges to a minimum. To prevent settling on local rather than global minima, 30 000 random directions are searched for a new minimum. More details can be found in Chiosi & Vallenari (2007).

4 THE HISTORY OF STAR FORMATION IN THE FIELD

4.1 NGC 2154

NGC 2154 is located in the NE border of the LMC ($\alpha = 5^{\rm h} 57^{\rm m} 38^{\rm s}$; $\delta = -67^\circ 15' 42''$; see Fig. 1 of this paper and fig. 12 of Costa et al. 2009). There are no previous determination of the SFH in this region.

As shown in Figs 5 and 6, our results indicate that the SFH in the field of NGC 2154 had bursts of star formation at 100–200 Myr, 400 Myr, 1–2 Gyr, 6 Gyr and 10 Gyr. We note that Olsen (1999), who studied the field SFR in six regions located mainly in the LMC bar, found bursts of star formation at 1 Gyr, 5 Gyr and at ages older
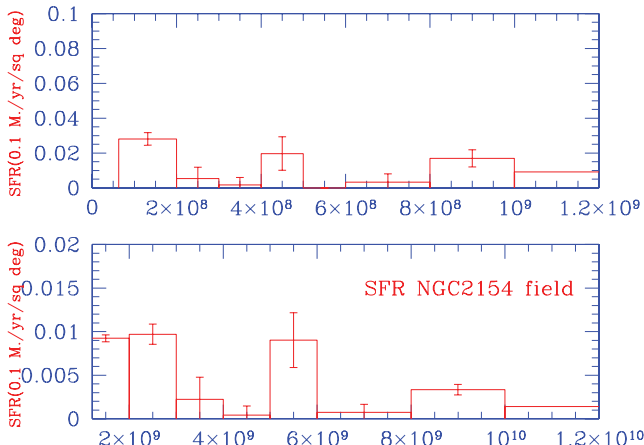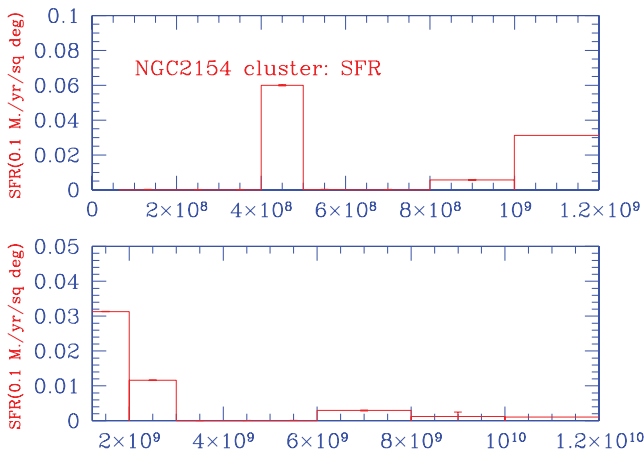
than 10 Gyr. These bursts of star formation are probably the result of dynamical interactions between the LMC and the Small Magellanic Cloud (SMC), at 200 Myr, and of the MCs with the Milky Way (MW), at 1.5 Gyr (Murai & Fujimoto 1986; Bekki & Chiba 2005). We note however that the validity of this statement cannot be tested at present because, given the uncertainties of the available proper motions measurements for the MCs (see e.g. Costa et al. 2009, 2011), their space motions are not precisely known (and hence the epochs of their peri-galactic passages and their past binding status are not well known – see Piatek, Pryor & Olszewski 2008).

Our results also show that, in agreement with those of Olsen (1999), the well-known gap in the cluster formation rate in the LMC, between 3 and 10 Gyr (Geisler et al. 1997; Balbinot et al. 2010), does not apply to the SFR of its field.

The age of NGC 2154 (1.7 Gyr, from Bau07) falls inside one of the peaks of the field SFH (1–2 Gyr). This is in agreement with Subramaniam (2004), who found that star and cluster formation rates in the LMC are anti-correlated in the age range 30–100 Myr, and correlated in the age range 300–1000 Myr and for ages of more than 1 Gyr.

As a check of the downhill-simplex algorithm we ran the star formation program on the NGC 2154 cluster area and tried to recover the age determination by Bau07. The result is that we find a main SF episode from 1 to 2 Gyr coincident with the previous determination plus a peak at 400 Myr probably due to the fact that the field population is not subtracted.

In Fig. 7 we compare the observed and synthetic CMDs of NGC 2154 field.

4.2 NGC 1898

NGC 1898 (= BSD99 2439) is located in the SW edge of the bar of the LMC ($\alpha = 05^{\rm h} 16^{\rm m} 41^{\rm s}\!24$; $\delta = -69^\circ 39' 24''\!.40$). Because this field is more crowded than that of NGC 2154, and because the observations were carried out in inferior seeing conditions, our data for NGC 1898 are 50 per cent complete at a brighter magnitude than those for NGC 2154 (50 per cent complete at $B = 20$ for the cluster area, and at $B = 22.5$ for the field).

As shown in Fig. 8, our results indicate that the SFH in the field of NGC 1898 had enhancements in the SFR at 200, 400, 800 Myr, similar to NGC 2154. Although not as notable as in the case of NGC 2154, a shallow peak is present at 6 Gyr (of the order of $0.002\,{\rm M}_\odot/{\rm yr}/{\rm square}$ degree). Consistent peaks are present at 2 and 8 Gyr. There is an important gap of 4–5 Gyr. We stress that we are not precise at ages older than 6 Gyr. This result is not inconsistent with those of Olsen (1999) for the LMC bar. Again, this peak and the other bursts of star formation seen in Fig. 8 are probably the result of dynamical interactions between the MCs, and of the MCs with the MW.

The peaks in the case of NGC 1898 are more consistent than in the case of NGC 2154 showing that the populations in the bar are much richer than those in the disc, as expected if star formation is proportional to mass density. But the relative intensity of young (<1 Gyr) and old (>1 Gyr) populations shows that old populations in NGC 1898 are much more abundant than in NGC 2154. In fact for a young population we have a factor 2 between NGC 1898 and NGC 2154 while for old population we have a factor 10. NGC 1898 is located in the bar while NGC 2154 is located in the disc. This is in agreement with Olsen (1999) who found a more conspicuous old component in the bar than in the disc.

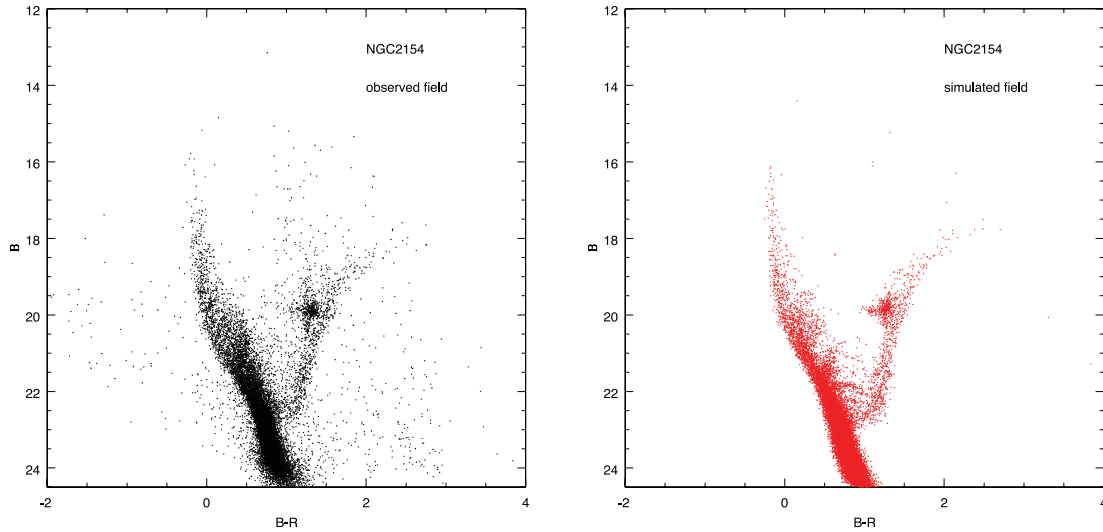In Fig. 9 we compare the observed and synthetic CMDs of NGC 1898 field.

Figure 5. SFR in the field around NGC 2154.

Figure 6. SFR for the cluster NGC 2154.

Figure 7. Observed and synthetic CMDs of the field around NGC 2154. The synthetic diagram is based on the SFR presented in Fig. 5.
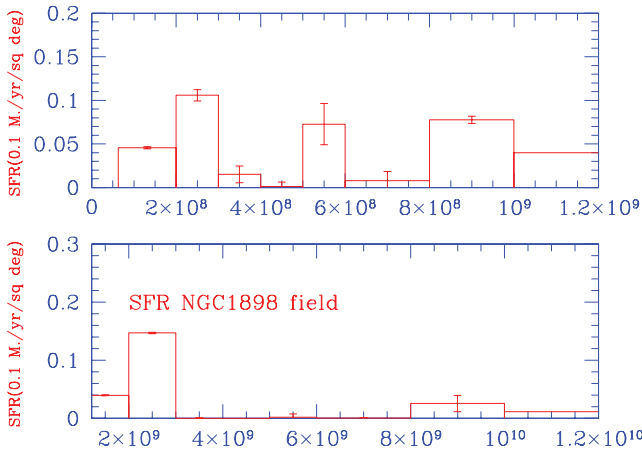

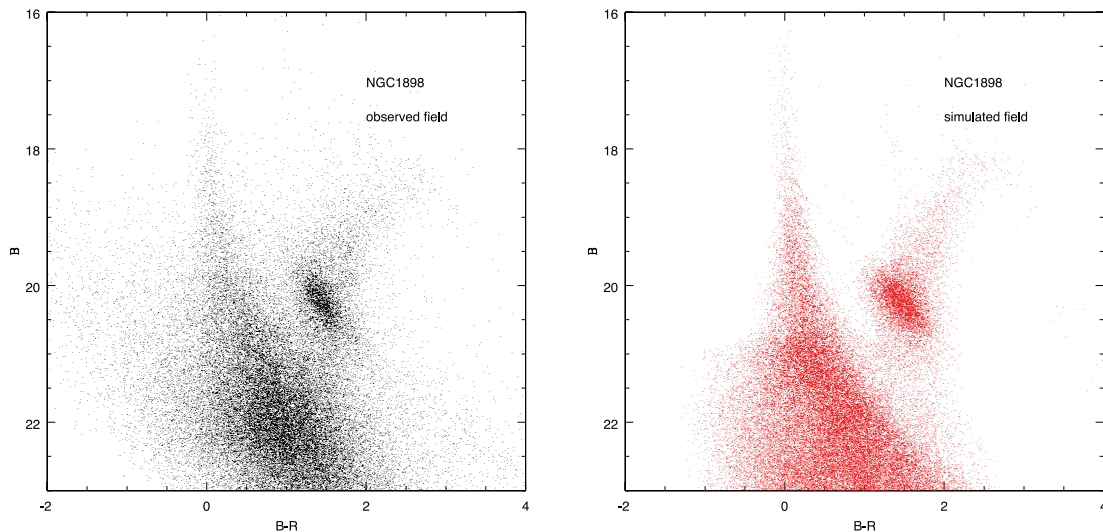**Figure 8.** SFR in the field around NGC 1898.

5 CLUSTER ANALYSIS IN THE FIELD OF NGC1898

The analysis of the NGC 1898 field showed the presence of small clusters. In the following, first we describe the procedure for determination of cluster parameters and then we discuss the relation with the field.

5.1 Cluster parameters

First, centres and radii needed to be determined for the clusters. The determination of cluster centres and radii was different for NGC2154 and for the other clusters in the NGC1898 area. In the first case the determination of the centre was done by visual estimation of the position of the peak density while the determination of the radius was done through the fit with Elson profiles (see Bau07). For the other small clusters in the NGC1898 area we tested several centres until we obtained the most clear case for a stellar concentration at the centre, and adopted as cluster centre the position of the peak density. The adopted sizes correspond to radii where
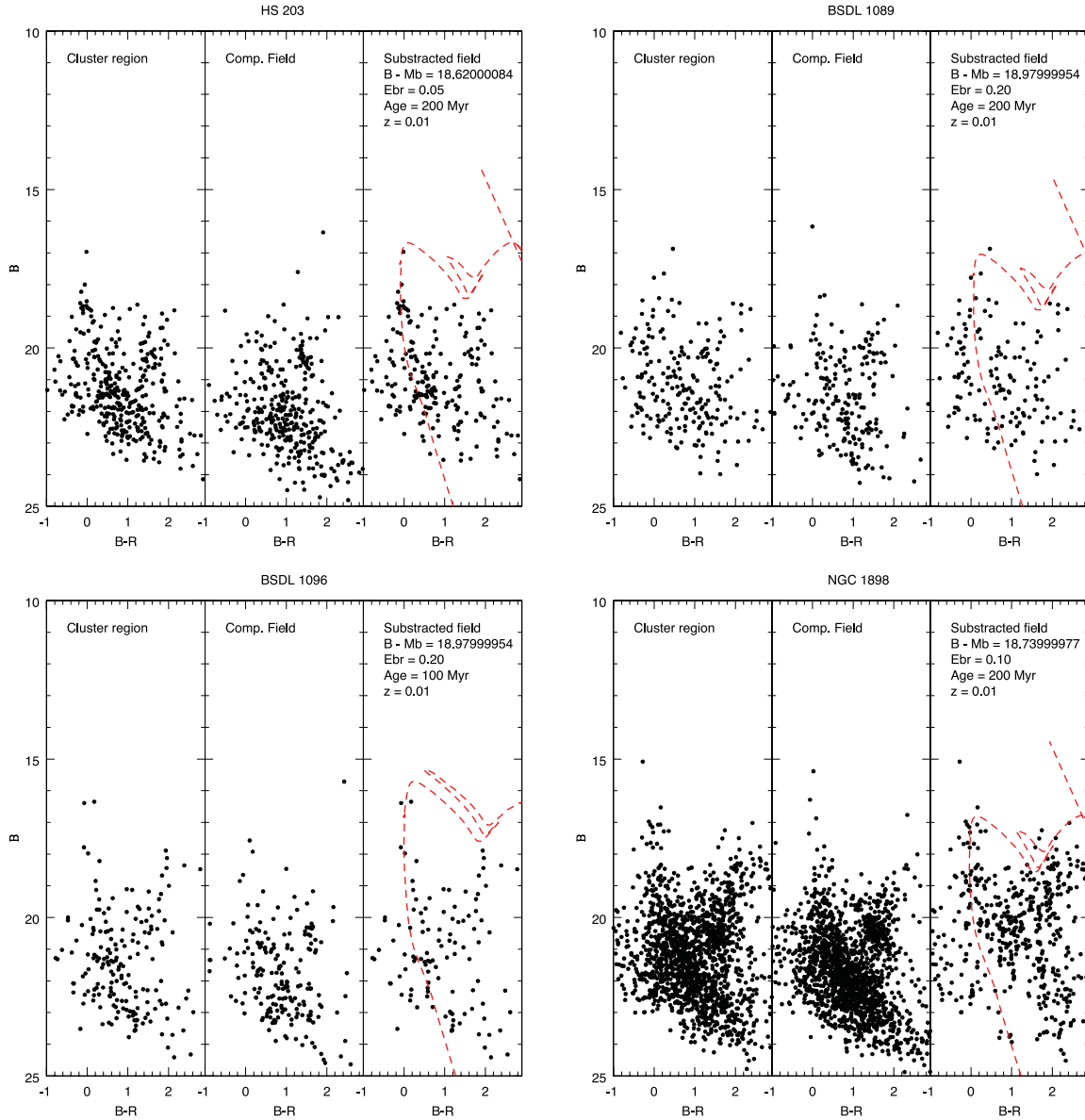

Figure 9. Observed and synthetic CMDs of the field around NGC 1898. The synthetic diagram is based on the SFR presented in Fig. 8.

Figure 10. Field star decontamination procedure for clusters HS 203, BDSL 1096 and NGC 1898. Left-hand panels are the CMDs of stars located in the *cluster regions*, central panels are the CMDs of stars in the corresponding *comparison regions*, and right-hand panels present the resulting *clean* CMDs. The dashed lines are the best-fitting isochrones, from Marigo et al. (2008). The cluster main parameters are indicated. For the diagrams of NGC 2154 refer to Bau07.

the densities get confused with the background level. In all cases, we considered only the brightest stars ($B < 21$) in order to avoid noise contamination by spurious detections. The resulting centre coordinates and radii are depicted with circles in Fig. 1 and given numerically in Table 2. The data presented for NGC 2154 in this table are from Bau07.

We then constructed *clean* CMDs of the clusters by selecting all stars located in each *clusterregion*, and in a *comparisonregion* of identical size, and statistically subtracting the latter from the former. This field star decontamination method is described in detail by Vallenari et al. (1992) and by Gallart et al. (2003). In Fig. 11 we present the result of carrying out this procedure on NGC 1898 and the seven small clusters. An equivalent result for NGC 2154 can be found in Bau07 (see their figs 8 and 9).

The bright part of each *clean* CMDs ($B < 19$) was compared with theoretical stellar evolutionary models from the Padova group

(Marigo et al. 2008) (see Figs 10 and 11), giving the age estimations indicated in Table 4. For all clusters in the region of NGC 1898 (see Fig. 1), we adopted a metallicity for the LMC of [Fe/H] = −0.30, in agreement with Rolleston, Trundle & Dufton (2002), which corresponds to $z = 0.010$. The $B − M_B$ and $E(B − R)$ values for each cluster are indicated in Figs 10 and 11. They are consistent with a distance modulus of 18.5, in agreement with Westerlund (1997). For the region of NGC 2154 we adopted the parameters indicated in Bau07. Some of the clusters like BSDL 1104 and BSDL 1096 are uncertain as they show few stars in the subtracted CMD.

Two distinct populations can be noticed: an older one (1–2 Gyr) exemplified by NGC 2154, and a younger one (100–200 Myr), exemplified by NGC 1898 and the seven small clusters. As explained in Section 4, we understand these two distinct populations as a result of bursts of star formation in the LMC.
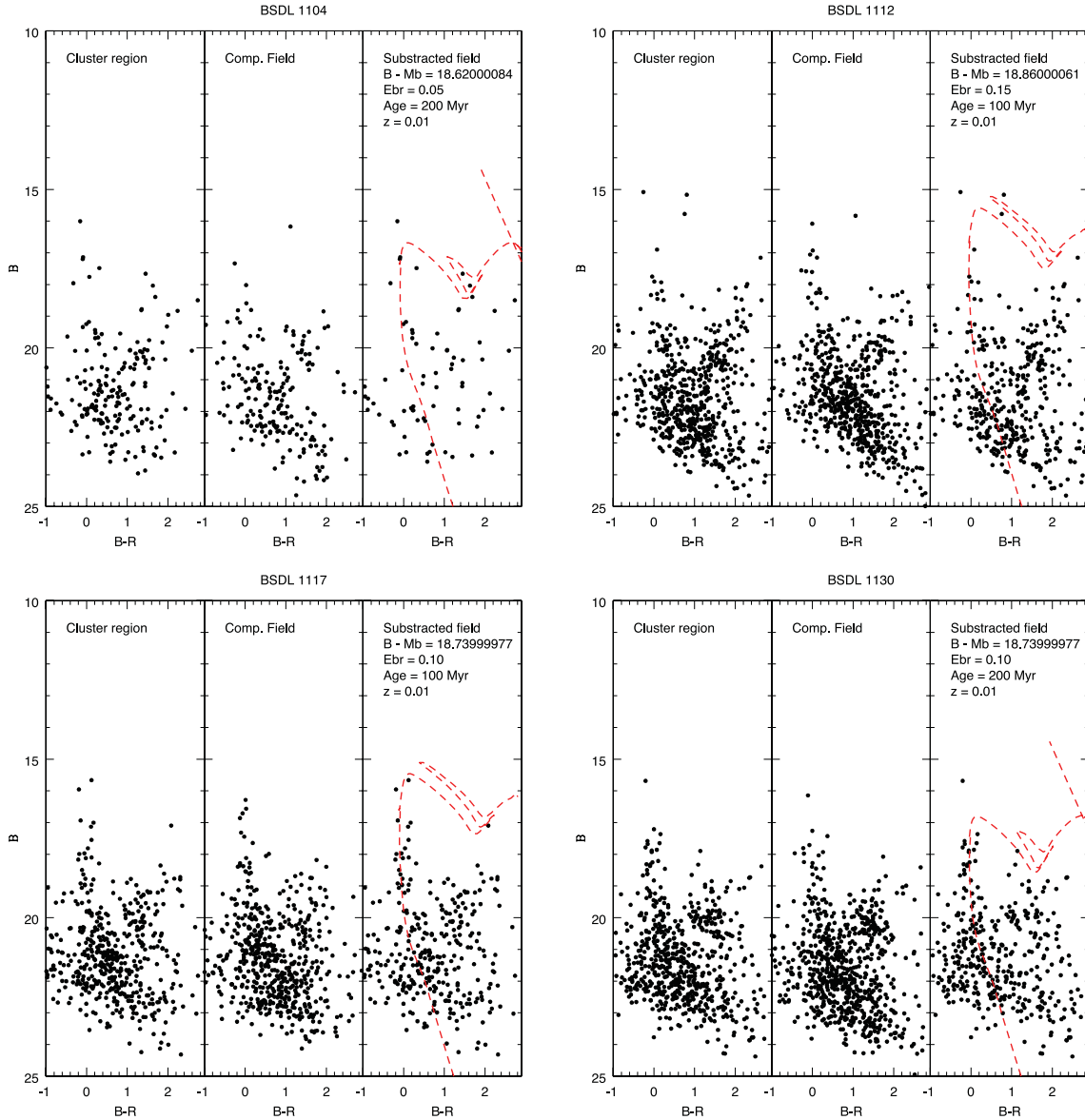
Figure 11. Field star decontamination procedure for clusters BDSL 1104, BDSL 1112, BDSL 1117 and BDSL 1130. Panels and lines have the same meaning as in Fig. 10, left-hand panels are the CMDs of stars located in the *cluster regions*, central panels are the CMDs of stars in the corresponding *comparison regions*, and right-hand panels present the resulting *clean* CMDs. The dashed lines are the best-fitting isochrones, from Marigo et al. (2008). The cluster main parameters are indicated. For the diagrams of NGC 2154 refer to Bau07.

Table 4. Parameters of the clusters investigated. We give the name, the position, the radius in arcmin, the age and the metallicity. Id_{B99} is simply the running number in the catalogue of Bica et al. (1999).* Cluster NGC 2154 presents a superposition of three stellar populations as discussed in Bau07.

Name	α_{2000}	δ_{2000}	Id_{B99}	R (arcmin)	Age (Myr)	z
HS 203	05:16:14.0	−69:49:32.0	2408	0.8 ± 0.1	200 ± 40	0.010
BSDL 1089	05:16:21.0	−69:36:03.0	2418	0.6 ± 0.2	200 ± 40	0.010
BSDL 1096	05:16:26.0	−69:40:28.0	2428	0.55 ± 0.1	100 ± 20	0.010
NGC 1898	05:16:42.0	−69:39:22.0	2439	1.6 ± 0.2	200 ± 40	0.010
BSDL 1104	05:16:43.0	−69:35:47.0	2443	0.55 ± 0.1	200 ± 40	0.010
BSDL 1112	05:16:57.0	−69:40:31.0	2464	1.0 ± 0.1	100 ± 20	0.010
BSDL 1117	05:17:10.0	−69:35:34.0	2473	0.9 ± 0.1	100 ± 20	0.010
BSDL 1130	05:17:28.0	−69:35:38.0	2498	1.0 ± 0.2	100 ± 20	0.010
NGC 2154	05:57:38.2	−67:15:40.7	6351	1.73 ± 0.2	1700*	0.005

5.2 Cluster population

The cluster analysis showed the presence of a coeval young (∼100–200 Myr) population of clusters spread around NGC 1898. This population corresponds to a peak in the SFH of the NGC 1898 field. The percentage of star formation happening in cluster relative to that taking place in the field is investigated by comparing the peak in the distribution of the global field to that of the subtracted field. The result does not show any significant change in the peak value possibly meaning that the SF at young ages takes place all over the area and is not concentrated on the cluster sites.

We note how the cluster and field populations are coeval. The field subtraction is a critical point in the definition of cluster ages through isochrone fitting. We recall that we cannot age older components in the clusters due to the depth of the photometry. So we probably identify the youngest episode of star formation happening both in clusters and field.

6 CONCLUSIONS

In this paper we investigated nine clusters of the LMC (NGC 2154, NGC 1898 and seven small clusters in the vicinity of the latter), and their related fields.

Two distinct populations of clusters were found: one cluster (NGC 2154) has a mean age of 1.7 Gyr, with an indication of extended star formation over roughly a 1 Gyr period (Bau07), while all others have ages between 100 and 200 My.

We also derived the SFRs for their adjacent fields. In the case of the NGC 2154 field, enhancements in the SFR are seen at 200, 400, 800 Myr, and in the case of the NGC 1898 field at 1, 6, 8 Gyr, with a notable gap of 4–5 Gyr between 1 and 6 Gyr. This implies that SFH proceeded in somewhat different ways in the two regions.

These bursts of star formation seem to be consistent with the dynamical interactions believed to have occurred between the LMC and the SMC at 200 Myr, and between the MCs and the MW at 1.5 Gyr.

ACKNOWLEDGMENTS

REFERENCES

Balbinot E., Santiago B. X., Kerber L. O., Barbuy B., Dias B. M. S., 2010, MNRAS, 404, 1625

Baume G., Carraro G., Costa E., Méndez R. A., Girardi L., 2007, MNRAS, 375, 1077 (Bau07)

Bekki K., Chiba M., 2005, MNRAS, 356, 680

Bica E. L. D., Schmitt H. K., Dutra C. M., Oliveira H. L., 1999, AJ, 117, 238

Bressert E. et al., 2010, MNRAS, 409, L54

Chiosi E., Vallenari A., 2007, A&A, 466, 165

Costa E., Méndez R. A., Pedreros M. H., Moyano M., Gallart C., Noël N., Baume G., Carraro G., 2009, AJ, 137, 4339

Costa E., Méndez R. A., Pedreros M. H., Moyano M., Gallart C., Noël N., 2011, AJ, 141, 136

Gallart C. et al., 2003, AJ, 125, 742

Geisler D., Bica E., Dottori H., Claria J. J., Piatti A. E., Santos J. F. C., Jr, 1997, AJ, 114, 1920

Girardi L., Bressan A., Bertelli G., Chiosi C., 2000, VizieR Online Data Catalog, 414, 10371

Holtzman J. A. et al., 1999, AJ, 118, 2262

Kroupa P., 2002, in Grebel E. K., Brandner W., eds, ASP Modes of Star Formation and the Origin of Field Populations Vol. 285, The Initial Mass Function and Its Variation. Astron. Soc. Pac., San Francisco, p. 86

Lada C. J., Lada E. A., 2003, ARA& A, 41, 57

Landolt A. U., 1992, AJ, 104, 340

Marigo P., Girardi L., Bressan A., Groenewegen M. A. T., Silva L., Granato G. L., 2008, A&A, 482, 883

Murai T., Fujimoto M., 1986, Ap&SS, 119, 169

Nelder J. A., Mead R., 1965, Comput. J., 7, 308

Noël N. E. D., Aparicio A., Gallart C., Hidalgo S. L., Costa E., Méndez R. A., 2009, ApJ, 705, 1260

Noël N. E. D., Gallart C., Costa E., Méndez R. A., 2007, AJ, 133, 2037

Olsen K. A. G., 1999, AJ, 117, 2244

Pagel B. E. J., Tautvaisiene G., 1998, MNRAS, 299, 535

Piatek S., Pryor C., Olszewski E. W., 2008, AJ, 135, 1024

Rolleston W. R. J., Trundle C., Dufton P. L., 2002, A&A, 396, 53

Rubele S. et al., 2012, A&A, 537, A106

Stetson P. B., 1987, PASP, 99, 191

Stetson P. B., 1992, in Butler C. J., Elliot I., eds, IAU Coll. 136, Stellar Photometry-Current Techniques and Future Developments. Cambridge Univ. Press, Cambridge, p. 291

Subramaniam A., 2004, A&A, 425, 837

Vallenari A., Chiosi C., Bertelli G., Meylan G., Ortolani S., 1992, AJ, 104, 1100

Westerlund B. E., 1997, Cambridge Astrophys. Ser. Vol. 29, The Magellanic Clouds. Cambridge Univ. Press, Cambridge

This paper has been typeset from a TEX/LATEX file prepared by the author.